Simulation of groundwater–seawater interactions in the Aral Sea basin by a coupled water balance model

JERKER JARSJÖ[1], IRINA ALEKSEEVA[2], CORINNA SCHRUM[3] & GEORGIA DESTOUNI[1]

1 *Dept of Physical Geography and Quaternary Geology, Stockholm University, SE-106 91 Stockholm, Sweden*
jerker.jarsjo@natgeo.su.se

2 *Institute of Oceanography, University of Hamburg, Center of Marine and Climate Research, Bundesstrasse 53, D-20146 Hamburg, Germany*

3 *Geophysical Institute, University of Bergen, Allégaten 70, N-5007 Bergen, Norway*

Abstract Large-scale irrigation has resulted in a dramatic shrinking and salinization of the Aral Sea. These changes also affect the groundwater discharge into the sea and the evaporative outflow from the sea surface. With the overall aim to quantitatively understand the processes governing the Aral Sea water balance and their effects on the groundwater discharge into the sea, we develop a 3-D coupled sea–groundwater budget model, forced by meteorological and river inflow data. The balance estimations performed indicate that the groundwater discharge into the sea must be between 2 and 6 km^3 $year^{-1}$. For the 15-year simulation scenarios considered, the groundwater inflow increases as the sea surface level drops. In addition, the model successfully reproduces seasonal cycling of the Aral Sea and predicts seasonal groundwater discharge fluctuations on top of the continuous long-term sea surface level drop.

Keywords Aral Sea; ECOSMO; groundwater; numerical modelling; sea model; water balance

INTRODUCTION

During the last century, increasing amounts of water were diverted to irrigated agricultural fields from the rivers flowing into the Aral Sea. This diversion caused a severe hydrological imbalance which has resulted in a dramatic shrinking and salinization of the Aral Sea (see e.g. Jarsjö & Destouni, 2004; Schrum & Alekseeva, 2005). The process started in the 1960s and has developed into one of the worst man-made environmental disasters ever. Because of the decreased river water inflow, the relative importance of groundwater discharge into the sea has increased considerably, and now constitutes a critical factor influencing the fate of the sea. This groundwater discharge is influenced by the ongoing sea surface level (ssl) lowering (by more than 20 m since 1960) associated with the sea's shrinkage (see e.g. Jarsjö & Destouni, 2004; Shibuo *et al.*, 2005). Since the Aral Sea is a terminal lake, the ssl lowering is in turn mainly governed by evaporation rates, which are also changing due to the sea shrinkage and due to regional climate changes caused by the desiccation of the sea. Hence, long-term groundwater flow predictions require a coupled balance modelling of the sea that allows for detailed meteorological forcing.

With the overall aim to quantitatively understand the processes governing the Aral Sea water balance changes and their effects on the groundwater discharge into the sea, we developed a three-dimensional coupled sea–groundwater budget model. In this coupled model, the inland boundary is defined through an upgradient constant-pressure boundary condition for the groundwater. Furthermore, the model is forced by data on river discharge and meteorological data for the sea region. The resulting groundwater discharge, ssl and coastline position then become parts of the model predictions.

MODEL DEVELOPMENT

A basis for the model coupling presented here is provided by the ECOSMO (ECOSystem MOdel) application for the Aral Sea region (Alekseeva *et al.*, 2004, 2005; Schrum & Alekseeva, 2005). This 3-D hydrodynamic sea–ice–groundwater model has 5-km horizontal resolution, 20 vertical *z*-levels and a 10-min time step. The sea-ice model scheme allows for wetting and drying of model cells in response to ssl variations as described by Schrum & Alekseeva (2005). It also provides a moving coastline, which serves as an internal interface between the sea and groundwater models. Since the groundwater model requires a finer grid (explained further after introducing equation (2)) a 500-m resolution was used here; it has been nested into the sea–ice model grid and the interactive exchange between model parameters has been organized via the interface of the coastline, which is represented at different resolutions in each of the models. The coupled model is forced with river runoff and atmospheric boundary conditions. The 6-hourly and 1.1 degree horizontal resolution ECMWF ERA-15 data (Gibson *et al.*, 1996) were used and small-scale turbulent air–sea fluxes (e.g. evaporation and heat fluxes) are re-calculated in the model using a scheme based on the Monin-Obukhov similarity theory. We here develop and employ a sea–groundwater budget model by excluding the thermo-hydrodynamic block of the hydrodynamic sea-ice model and including instead the evaporation rates from a corresponding previous run of the full model. This considerably reduces the computer time for the calculations (a 3-hour time step was chosen) and still retains the governing processes of the water balance.

The main task of the groundwater module is to predict regional changes in groundwater discharge into the sea in response to the sea surface lowering. We then assume that the regional groundwater flow is essentially linear and that storage is negligible. Under these conditions, the simple and analytical groundwater relations of Jarsjö & Destouni (2004) follow from direct application of Darcy's law along the regional flow direction. The resulting relation for the hydraulic gradient:

$$j / j_0 = \frac{X_{bound}(z_{bound} - d_{gw} - z_{sea})}{(X_{bound} + X_{sea})(z_{bound} - d_{gw} - z_{sea,0})} \tag{1}$$

is applicable along the coast and could therefore be implemented in the sea model. In equation (1), X_{bound} [L] is the distance from the original sea shore to the assumed groundwater model boundary, where the groundwater table will be relatively unaffected by the sea surface lowering (with the distance being measured along the

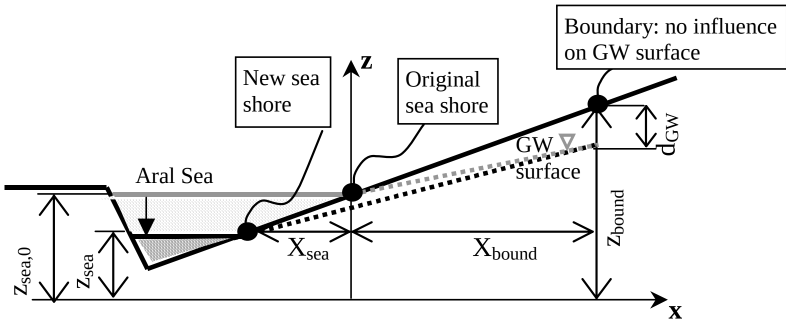

Fig. 1 Illustration of the distances X_{bound}, d_{gw}, z_{bound}, z_{sea} and X_{sea}. After Jarsjö & Destouni (2004).

regional flow direction); d_{gw} [L] is the depth to the groundwater table at the boundary; $z_{sea,0}$ is the initial sea surface level; z_{sea} [L] is the varying sea surface level during the simulation; X_{sea} [L] is the sea retreat, i.e. the distance between the considered coastal cell and the original sea shore; j is the hydraulic gradient for the cell during the sea shrinkage process (i.e. for $X_{sea,I} \neq 0$ and $z_{sea} \neq z_{sea,0}$); and j_0 is the initial hydraulic gradient before the start of shrinkage (i.e. for $X_{sea,I} = 0$ and $z_{sea} = z_{sea,0}$). The distances X_{bound}, d_{gw}, z_{bound}, z_{sea} and X_{sea} are shown in Fig. 1.

Furthermore, the regional groundwater discharge into the sea, Q_i^{GW} [L^3 T^{-1}], is proportional to the initial (pre-1960) groundwater discharge and the average regional j/j_0 ratio according to:

$$Q_i^{GW} = \frac{Q_i^{GW0}}{ncell_i} \sum_{cell_i} j/j_0 \tag{2}$$

in which subscript i refers to region number (see Table 1 and Fig. 2), Q_i^{GW0} [L^3 T^{-1}] is the initial regional groundwater discharge into the sea before shrinking (for $X_{sea,I} = 0$ and $z_{sea} = z_{sea,0}$), $ncell_i$ is the number of coastal cells within region i, and the summation is performed over all the coastal cells of region i. The initial regional discharges Q_i^{GW0} are obtained on the basis of independent estimates of the total groundwater discharge into the Aral Sea, Q^{GW0}, and the regional coastal lengths (see Table 1 and the associated descriptive text).

Through the model coupling, the groundwater module receives updated values of z_{sea} from the sea module. Furthermore, a coastline vector (consistent with the z_{sea} elevation isoline) is calculated for each time step, based on the fine-grid topography model; for accurate application of groundwater equations (1) and (2) to the partly steep topography of the Aral Sea basin, the spatial resolution needs to be high. The coastal cell X_{sea}-values are determined through a pre-processing step, where an input X_{sea}-matrix is created, yielding for each cell the distance between the cell and the original coastline. This X_{sea}-matrix is then used in combination with the current coastline vector for the determination of regional groundwater discharges to the moving coastline. The X_{sea}-matrix pre-processing was conducted considering each of the 16 regions (Table 1), using ESRI-ArcGIS (v 8.3) and the distance function in Spatial Analysist package, with the resulting distances for all 16 zones shown in Fig. 2.

Table 1 Boundary conditions for the regions considered. The distance from the coastline to the groundwater model boundary X_{bound} is 200 km in all cases, and $z_{sea,0} = 0$. The assigned initial groundwater flow within each zone relative to the total initial groundwater flow is assumed to be equal to the coastal length within the zone relative to the total coastal length $L_i^0/\Sigma L_i^0$.

Region number	$d_{gw,i}$[a]	Land elevation (m) at boundary, $z_{bound,i}$	L_i^0 (km)[b]	$L_i^0/\Sigma L_i^0$ (%)	**Region number** (cont'd)	$d_{gw,i}$[a]	Land elevation (m) at boundary, $z_{bound,i}$	L_i^0 (km)[b]	$L_i^0/\Sigma L_i^0$ (%)
1	3	40	53.3	5.5	**9**	50	96	38.7	4.0
2	3	40	54.6	5.6	**10**	50	96	36.1	3.7
3	3	40	48.5	5.0	**11**	50	96	55.9	5.8
4	3	40	30.5	3.1	**12**	50	96	50.5	5.2
5	3	40	33.5	3.5	**13**	50	96	71.8	7.4
6	3	40	92.9	9.6	**14**	50	96	83.5	8.6
7	50	96	167.7	17.3	**15**	3	40	69.9	7.2
8	50	96	27.5	2.8	**16**	3	40	56.1	5.8
								Σ971.1	Σ100

[a] Depth (m) to groundwater at boundary.

[b] Initial coastal length, measured along a line oriented perpendicular to the regional groundwater flow direction at the location of the original shore (dashed line in figure).

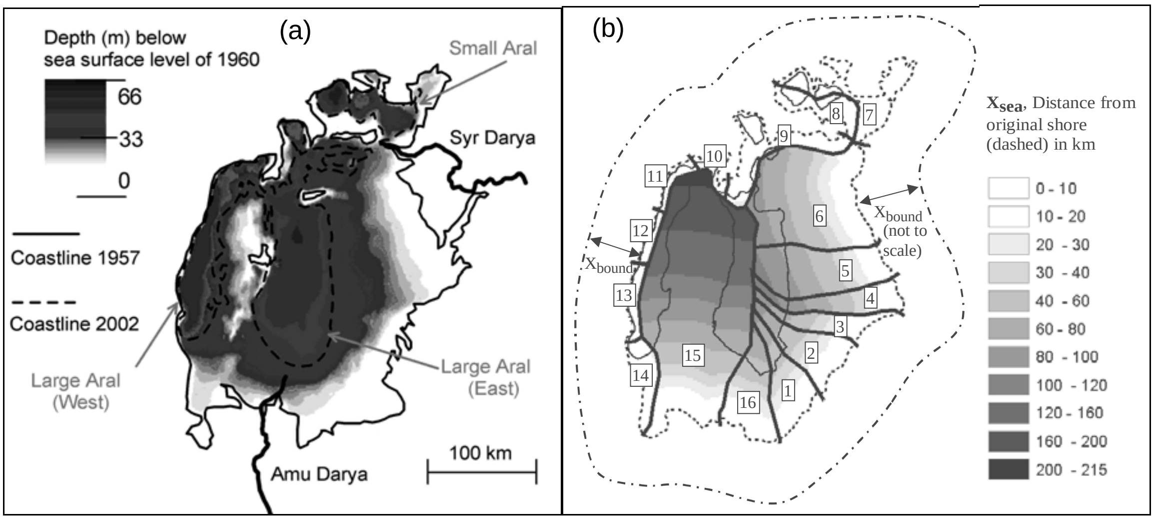

Fig. 2 (a) Model topography, and (b) the 16 regions of the Aral Sea considered in the groundwater model, and regional distances, along the mean groundwater flow direction, to the 1975 coastline.

SITE DESCRIPTION

Figure 2(a) shows a topographic map of the shrinking Aral Sea, including the pre-1960 coastline (solid line) and a recent coastline (2002). Figure 2(b) also shows the location of the 16 numbered regions of the groundwater model. We consider the time period 1979–1993, during which the Aral Sea split into two separate water bodies, the Small Aral and Large Aral.

The site-specific values and relations assumed for the groundwater variables X_{bound}, z_{bound}, and d_{gw}, representing the regional boundary conditions, are shown in

Table 1; see Jarsjö & Destouni (2004) for an extended discussion on groundwater boundary conditions in the Aral Sea vicinity. Furthermore, the total, initial groundwater inflow Q^{GW0} value was determined through calibration (see the results section) and distributed among the 16 considered regions (see Fig. 2) on the basis of their initial coastal extents (or lengths) in region *i*, L_i^0 perpendicular to the regional groundwater flow direction, according to $Q_i^{GW} = Q^{GW0}\, L_i^0/\Sigma L_i^0$ (see Table 1).

RESULTS AND DISCUSSION

In 1991, two separate lakes formed in the Large Aral and Small Aral basins. After 1991, the model scenarios primarily consider the conditions in the Large Aral basin. The basic numerical experiment illustrated in Fig. 3(a) was performed using external model parameters, such as river runoff and precipitation, from the study of Alekseeva *et al.* (2005). The evaporation rates were estimated using the previously described hydrodynamic sea-ice model, shown to produce reliable evaporation rates that agree well with independent estimations (Schrum & Alekseeva, 2005).

However, Schrum & Alekseeva (2005) argue that the river runoff and precipitation have great uncertainties and might be overestimated. Therefore, in an alternative scenario we reduce both the river and precipitation contributions to the water balance by 50%. In both cases, we treat the initial groundwater flow value (Q^{GW0}) as a fitting parameter and adjusted it to achieve matching between the modelled sea surface level (ξ-line in Fig. 3(a)) and the observed values in the Aral Sea (filled circles in Fig. 3(a); regarding the Large Aral after its formation in 1991). The associated (total) groundwater inflow to the Aral Sea then varies from the adjusted initial inflow of 2 km^3 year^{-1} up to 2.3 km^3 year^{-1} in 1990. The solid lines in Fig. 3(b) illustrate the groundwater inflow to the large Aral basin (L-line in Fig. 3(b)) and to the small Aral basin (S-line in Fig. 3(b); this simulation stops in 1991 when the Small Aral and Large Aral formed separate seas).

For each of the basic and alternative scenarios, the sum of the L-line and S-line in Fig. 3(b) then quantifies the total groundwater inflow to the Aral Sea before

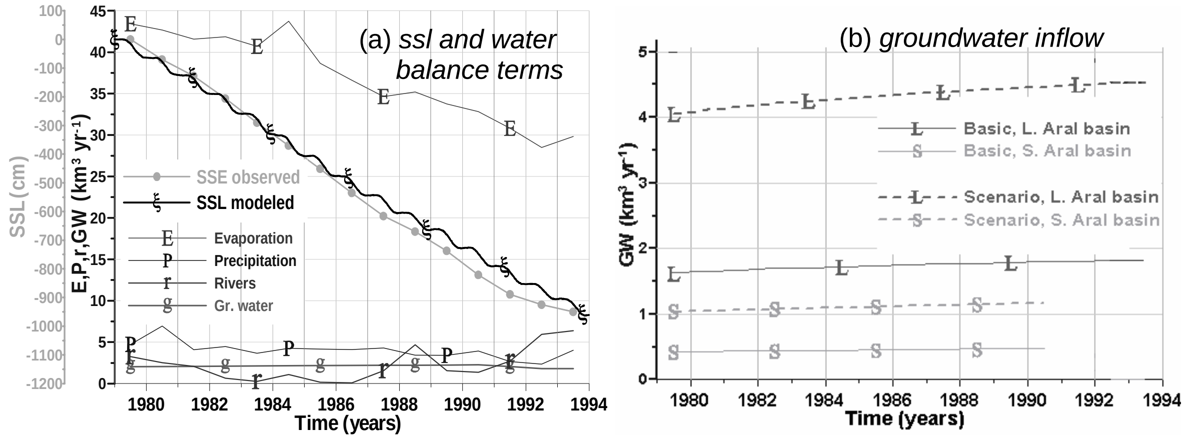

Fig. 3 Model results for: (a) ssl including all the water balance terms of the basic experiment, and (b) groundwater inflow in the basic experiment (solid lines) and the alternative scenario (dashed lines).

1991 (i.e. before the two separate seas formed). The dashed lines in Fig. 3(b) illustrate the corresponding groundwater results for the alternative scenario (not shown in Fig. 3(a)), for which the resulting total groundwater inflow varies between 5 and 5.5 km^3 year^{-1}. Figure 3(b) shows that for both scenarios, the total groundwater inflow increases slightly with time, as a (hydraulic) response to the sea surface lowering.

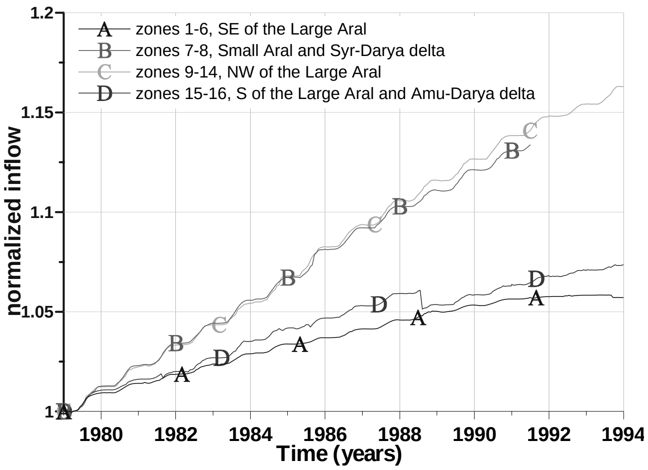

Fig. 4 Groundwater inflow to each zone normalized by corresponding initial inflow.

Figure 4 illustrates the basic experiment and shows the relative changes in groundwater inflow for different geographical parts of the Aral Sea basin, where the flows are normalized with respect to the conditions in 1979 (at the start of the simulation). For the southeastern part of the Large Aral as well as its southern part with the Amu Darya delta (curves A and D in Fig. 4), the increase in groundwater inflow is relatively small during the simulation. In contrast, for the northwestern part of the Large Aral and the Small Aral with the Syr-Darya delta (curves B and C of Fig. 4), the changes are more considerable, with an average increase of more than 15% between 1979 and 1993. Since the sea surface lowering has continued since 1993, one can expect a corresponding further increase in groundwater inflow to the western basin, whereas the groundwater inflow to the eastern basin, which may soon (after 2005) constitute a separate lake, remains essentially unchanged. The inter-annual oscillations in groundwater inflow, seen e.g. in curves B and C of Fig. 4, reflect seasonal fluctuations of the Aral Sea surface level and its water budget.

In summary, the sea–groundwater budget model developed here successfully reproduces seasonal cycling of the Aral Sea on top of the continuous sea surface level drop, and associated area and volume decrease, for the 15-year simulation period considered. Considering the uncertainties in the precipitation data and river flow data, the water balance estimates indicate that the groundwater discharge into the sea must be between 2 and 6 km^3 year^{-1}. The predicted long-term trends of increasing regional groundwater inflow are consistent with the previous groundwater model results of Jarsjö & Destouni (2004), where a simplified (hydraulic) model was used in combination with ssl data. Hence, the developed model provides a powerful tool for closer investigation of governing water balance processes and associated regional groundwater flows at different time scales.

REFERENCES

Alekseeva, I., Schrum, C. & St. John, M. (2004) ECOSMO, a coupled ecosystem model of the North Sea and Baltic Sea Part I: Model description and simulation of annual characteristics in the North Sea (manuscript in preparation for submission to *J. Marine Systems*).

Alekseeva, I., Jarsjö, J., Schrum, C. & Destouni, G. (2005) Coupled 3D sea-ice-groundwater model. On the role of groundwater for the Aral Sea water and salt budget (manuscript in preparation for submission to *J. Marine Systems*).

Gibson, R., Kallberg, P. & Uppala, S. (1996) The ECMWF Re-Analysis (ERA) project. *ECMWF Newsletter* **73**, 7–17.

Jarsjö, J. & Destouni, G. (2004) Groundwater discharge into the Aral Sea after 1960. *J. Marine Systems* **47**, 109–120.

Schrum, C. & Alekseeva, I. (2005) The Aral Sea water and salt budget estimations from a 3D coupled sea-ice model ECOSMO (manuscript in preparation for submission to *J. Geophys. Res*).

Shibuo, Y., Jarsjö, J. & Destouni, G. (2005) Modelling groundwater-seawater interactions in the Aral Sea region. In: *Groundwater and Saline Intrusion: Selected papers from the 18th Salt Water Intrusion Meeting* (ed. by L. Araguás, E. Custodio & M. Manzano), 163–171. Instituto Geológico y Minero de España, Madrid, Spain. ISBN: 84-7840-588-7.